FATIGUE STRENGTH ASSESSMENT OF A SHORT FIBRE-REINFORCED PLASTIC BASED ON THE ENERGY DISSIPATION

G. Meneghetti*, M. Quaresimin, M. De Monte*****
Department of Mechanical Engineering – University of Padova,
****Department of Management and Engineering – University of Padova***
*****Robert Bosch GmbH - Corporate Research (CR/APP2), Waiblingen (Germany)***

Keywords: **short fibre composites, infrared thermography, fatigue, energy dissipation**

Abstract

An energy-based approach is proposed for fatigue analysis of specimens weakened by rounded notches. The energy dissipated as heat by a unit volume of material per cycle is assumed as fatigue damage indicator. A theoretical model based on the energy balance is presented, where the different forms of energy exchanged in a fatigue test are involved. An experimental technique which enables one to estimate the proposed energy parameter is presented and applied to the analysis of the fatigue behaviour of a short fibre-reinforced plastic. The limits of applicability of the presented approach is also discussed.

1 Introduction

The thermographic approach adopted to estimate the fatigue limit of metals [1] and the high cycle fatigue strength (HCFS) of composites [2-3] is well documented in literature. Such an approach is based on the experimental observation that during a fatigue test the surface temperature of a material increases, such that the higher the applied stress amplitude the higher the temperature increase [4-5], as depicted in Fig. 1. Once the stationary thermal rises have been experimentally measured, the HCFS of the material $\sigma_{0,th}$ can be determined by extrapolation of the best fitting curve that correlates the applied stress amplitudes σ_a and the stationary temperature increments ΔT_{stat} [1, 23], as depicted in Fig. 2a. According to a slightly different procedure [1, 3, 6], the reference HCFS of the material should be estimated by intersecting the two straight lines that interpolates the experimental data reported in the form shown by Fig. 2b for low and high stress amplitudes.

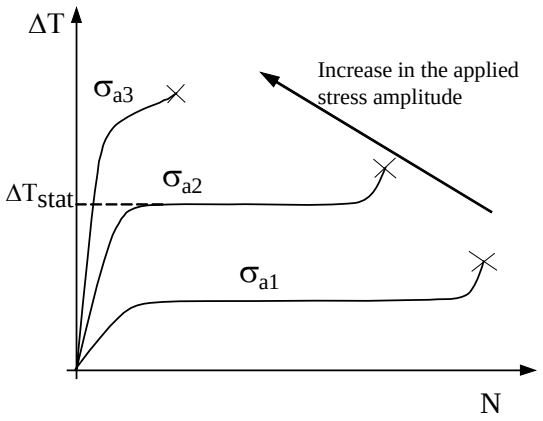

Fig. 1. Schematic view of the temperature increase of different specimens undergoing a fatigue test.

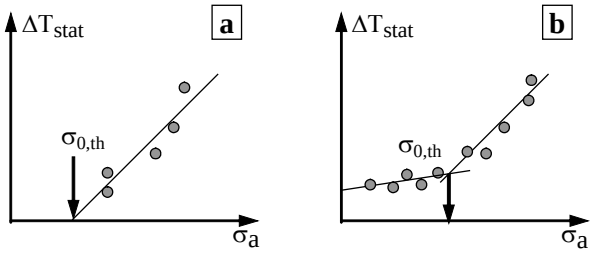

Fig. 2. Experimental estimation of fatigue limit (for metals) and high cycle fatigue strength (for composites) according to the thermographic methods.

It should be noted that in the case of metallic materials temperature is not an indicator of fatigue damage by nature. In fact some temperature rise can be measured in specimens cyclically loaded even below the fatigue limit [1, 6, 7]. Nonetheless it has been highlighted [8] that, dealing with fatigue of low carbon steels, in an experimental test conduced on a single specimen by progressively increasing the applied stress amplitude, the slope of the curve fitting the experimental data ΔT_{stat}-σ_a shows a sharp variation at the stress level that generates the first slip band. It is well known [9,10] that such a stress

level is close to the fatigue limit, even if they do not coincide from a scientific point of view, since the fatigue limit corresponds to a slightly higher stress level, at which an initiated micro-crack stops propagating when reaching the first microstructural barrier.

On the other hand in the case of composite materials, due to the different damage mechanics, temperature changes can provide useful information about location, extension and evolutions of damage under static and fatigue loading, see Refs. 5, 11-17 for some examples. In the case of fatigue loading of short fibre, thermoplastic matrix composites, damage mechanisms like fibre-matrix debonding, fibre pull-out and matrix cracking can act even at low stress level; the resulting damage associated to the visco-elasto-plastic behaviour of the matrix generate a significant amount of heat which is converted in significant temperature increases even for stress well below the high cycle fatigue strength of the material. This behaviour justifies the need for using the thermographic procedure in figure 2b in the case of composites.

Whether or not temperature represents a true indicator of the fatigue damage, thermometric methods proved to be able to estimate the fatigue limit of materials and components in a reasonably good agreement with the traditional methods such as the stair-case procedure.

Recently an experimental thermometric approach supported by a theoretical model has been proposed for an engineering analysis of the fatigue strength of materials and components [18]. The fatigue damage indicator is assumed to be the energy (rather than the temperature) released by the material as heat in a unit volume and per cycle. The specific energy dissipated during a fatigue test is derived from the experimental measurement of the surface temperature at the critical point and is supported by a theoretical model based on the energy balance.

Then, aims of this work are the following:

- to summarise the experimental energy-based approaches proposed in the literature for fatigue strength assessments of materials and components;
- to summarise the theoretical model for estimating the specific energy released by the material as heat in an experimental test;
- to apply the theoretical model to correlate the fatigue strength of smooth and notched specimens made of a short fibre-reinforced composites.

2 Experimental energy-based methods for fatigue strength assessments

It has been highlighted [18] that temperature is not a promising parameter for fatigue strength estimations, at least for metals. In fact temperature distribution in a specimen made of a given material depends on the specimen geometry, the test frequency, and the boundary conditions that defines the heat transfer rate from the specimen to the surroundings (one important factor among these is the room temperature). As an example, consider a smooth specimen having a constant cross section along its length. When subjected to cyclic loading a temperature rise will occur, which is not uniform along specimen's length. In fact the specimen behaves, as a first approximation, like a bar subjected to a uniform heat generation along its length and heat dissipation at the specimens ends: then temperature distribution will be parabolic along the specimen's longitudinal axis. If temperature were a fatigue damage indicator, failure should invariably occur at the specimen mid-section, which is not true in general. Conversely, the energy dissipated in a unit volume of material per cycle is constant along the specimen's axis.

In the literature there are a number of experimental energy-based approaches for fatigue strength assessment of material and components. According to different Authors, different forms of energy are considered as fatigue damage indicators, i.e. the mechanical energy expended during the fatigue test, the energy stored with in the material and the energy dissipated as heat.

The expended mechanical energy measured by the area of the hysteresis loop was assumed as a fatigue damage index by Feltner and Morrow [19]. Halford [20] correlated the work expended for a unit volume of material to the fatigue life of a variety of metal materials. In particular it was shown that fatigue is a very dissipative phenomenon since in the medium cycle fatigue one hundred time more plastic strain hysteresis energy is dissipated than in a monotonic test up to failure. The strain hysteresis energy concept has more recently been adopted by Charkaluk [21] in the context of strength assessments under thermomechanical loadings and by Klingbeil [22] in the area of Fracture Mechanics studies.

Kaleta et al. [7] assumed the stored energy within the material (the so-called 'stored energy of cold work') as a fatigue damage index. After overcoming some experimental difficulties, they measured the stored energy as difference between

the expended mechanical energy and the energy converted into heat. Risitano and co-workers [24] proposed the use of a parameter derived from the experimental measurement of the surface temperature, which has been correlated to the stored energy after failure. Moreover such a parameter has been assumed as a material constant at fatigue failure.

Reifsnider and Williams correlated heat generation and development of fatigue damage in boron-aluminium and boron-epoxy composites [11]

Gamstedt et al. assumed heat dissipation as a damage parameter when analysing the fatigue behaviour of Angle-Ply and UD hybrid laminates [13]. Similar approaches were adopted in Refs. 16 and 17. It is worth noting that although frequently used for damage characterisations during fatigue testing, at the best of author' knowledge, energy-based approaches were never used so far for fatigue strength assessments in composites.

In the present work we adopt heat dissipation in order to correlate the fatigue strength of smooth and notched specimens in a short fibre-reinforced plastic. It is believed that heat dissipation is easier to be measured rather than the expended mechanical energy and the stored energy of cold work, especially when high cycle fatigue regime is considered.

In the next section the theoretical model will be briefly summarised.

3 The theoretical model for fatigue life estimation based on the energy dissipation

The proposed model [18] is based on the energy balance of a control volume V of material undergoing a fatigue test, as depicted in Fig. 3. The statement of the first law of thermodynamics is:

input mechanical energy (W) = dissipated thermal energy (Q) + variation of the internal energy (ΔU)

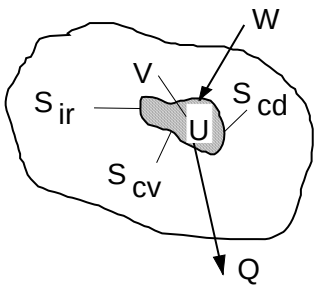

Fig. 3. Energy balance of a material undergoing a fatigue test [18].

$$\begin{aligned}
&\int_V \left(\oint \sigma_{ij}\cdot d\varepsilon_{ij}\right)\cdot f\cdot dV = \\
&\int_{S_{cd}} -\lambda\cdot \mathrm{grad}\vec{T}\cdot\vec{n}\cdot dS_{cd} + \\
&\int_{S_{cv}} \alpha\cdot(T-T_\infty)\cdot dS_{cv} + \\
&\int_{S_{ir}} \kappa\cdot\sigma_n\cdot\left(T^4-T_\infty^4\right)\cdot dS_{ir} + \\
&\int_V\left(\rho\cdot c\cdot\frac{\partial T}{\partial t}+\dot{E}_p\right)\cdot dV
\end{aligned} \qquad (1)$$

where σ_n is the Stephan-Boltzmann constant equal to $5.67\cdot10^{-8}$ W/(m$^2\cdot$K^4), $\mathrm{grad}\vec{T}$ is the gradient of the temperature field, λ is the thermal conductivity, ρ is the material density, c is the material specific heat, n is the outward unit normal, κ is the surface emissivity, T_∞ is the room temperature and t is time. The dissipated thermal energy is described by the three heat transfer mechanisms operating through the surface S, i.e. conduction (cd), convection (cv) and radiation (ir). The rate of variation of the internal energy contains two terms: the first one describes the transient material thermal variations while the second term represents the rate of accumulation of the 'stored energy of cold work', which is responsible for changes in material microstructure leading to initiation of fatigue micro-cracks.

By transforming the surface integral of the conduction term into a volume integral, we have :

$$-\lambda\cdot\int_{S_{cd}}\mathbf{grad}\vec{\mathbf{T}}\cdot\vec{\mathbf{n}}\cdot dS_{cd} = -\lambda\cdot\int_V \mathrm{div}\left(\mathbf{grad}\vec{\mathbf{T}}\right)\cdot dV$$

where:

$$\mathrm{div}\left(\mathrm{grad}\vec{T}\right)=\nabla^2 T \quad\rightarrow\quad \nabla^2 T=\frac{\partial^2 T}{\partial x^2}+\frac{\partial^2 T}{\partial y^2}+\frac{\partial^2 T}{\partial z^2}$$

the energy balance equation in integral form can be written as:

$$\begin{aligned}
&\int_V \left(\oint \sigma_{ij}\cdot d\varepsilon_{ij}\right)\cdot f\cdot dV = \\
&\int_V -\lambda\cdot\nabla^2 T\cdot dV + \\
&\int_{S_{cv}} \alpha\cdot(T-T_\infty)\cdot dS_{cv} + \\
&\int_{S_{ir}} \kappa\cdot\sigma_n\cdot\left(T^4-T_\infty^4\right)\cdot dS_{ir} + \\
&\int_V\left(\rho\cdot c\cdot\frac{\partial T}{\partial t}+\dot{E}_p\right)\cdot dV
\end{aligned} \qquad (2)$$

It has been shown that if we consider a smooth specimen having a constant cross section, the temperature variation across the section itself, that is in the x and y direction in Fig. 4, can be neglected [18]. Then, by noting that dV=A·dz, eq. (2) can be written in differential form as:

$$\left(\oint \sigma_{ij} \cdot d\varepsilon_{ij}\right) \cdot f = -\lambda \cdot \nabla^2 T + \alpha \cdot (T - T_\infty) \cdot \frac{p}{A} + \sum_i (\kappa_i \cdot \ell_i) \cdot \frac{\sigma_n}{A} \cdot \left(T^4 - T_\infty^4\right) + \left(\rho \cdot c \cdot \frac{\partial T}{\partial t} + \dot{E}_p\right) \quad (3)$$

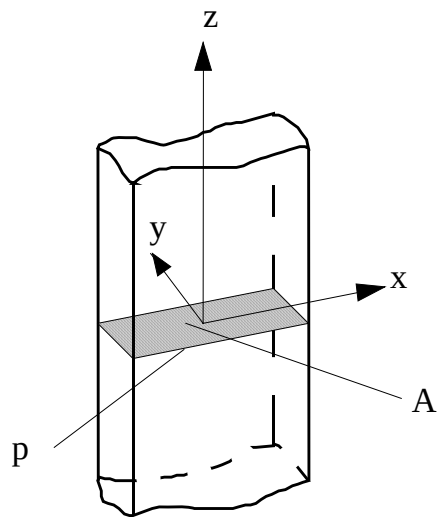

Fig. 4. Frame of reference adopted in the energy balance (Eq. (3)).

Allowing for thermal steady state conditions to be reached after a certain period of time is elapsed from the beginning of the experimental test, eq. (3) can be rewritten as follows:

$$\left(\oint \sigma_{ij} \cdot d\varepsilon_{ij}\right) \cdot f = H + \dot{E}_p \quad (4)$$

being H equal to:

$$H = -\lambda \cdot \nabla^2 T + \alpha \cdot (T - T_\infty) \cdot \frac{p}{A} + \sum_i (\kappa_i \cdot \ell_i) \cdot \frac{\sigma_n}{A} \cdot \left(T^4 - T_\infty^4\right) \quad (5)$$

H represents the thermal power dissipated per unit volume of material by means of the three heat transfer mechanisms.

Eq. (5) can be solved after tentatively assigning H and comparing the obtained T(z) temperature distribution with the experimental one, as measured by means of an infrared camera. By adopting such an experimental technique to monitor fatigue tests conduced on smooth specimens made of a commercial stainless steel and a nodular cast iron [25], it has been found that all three heat transfer mechanisms contribute to the heat dissipation with the same order of magnitude, but conduction is the prevailing mechanism being the relevant rate of heat transfer up to 80 % of the total, in particular in the medium and low cycle fatigue regime. Of course such results are meant to be specific to the particular materials and testing conditions analysed in Ref. 25.

When dealing with notched specimens and real components, the one-dimensional form of eq. (5) cannot be applied any longer. Under such geometrical conditions, being valid the stationary assumption previously made, eq. (4) holds true. It has been shown [18], that the energy dissipated as heat Q in a unit volume of material and per cycle can be evaluated by experimentally measuring the cooling rate of the material after a sudden interruption of the fatigue test. The procedure is depicted in Fig. 5.

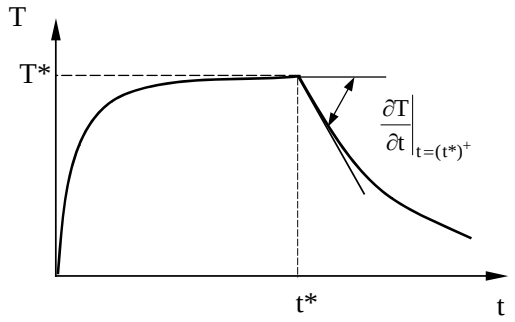

Fig. 5. Temperature gradient as measured after suddenly stopping the fatigue test at t=t*.

In fact, by so doing the mechanical input power (represented by the left-hand side of eq. (4)) and the rate of accumulation of plastic strain E_p in Eq. (4) will drop to zero, so that it can be written:

$$\rho \cdot c \cdot \left.\frac{\partial T}{\partial t}\right|_{t=(t^*)^+} = -\left(H_{cd} + H_{cv} + H_{ir}\right) \quad 6)$$

where the thermal power H dissipated per unit volume of material does not change just before and just after the time t* (at which the test is interrupted), because it depends only on the temperature distribution and on the room temperature, which do not change through the time t*. Then, the specific energy loss Q can be simply derived by knowing the load frequency f:

$$Q = \frac{H}{f} \qquad 7)$$

4 Material and fatigue test results

Fatigue tests were conduced on plain and notched specimens in 5-mm-thick PA66-GF35 material, i.e. a 35% wt. short glass fiber reinforced polyamide composite, with the nominal fibre orientation aligned with the specimen longitudinal axis. The thermophysic properties were provided by the manufacturer; in particular the material density resulted equal to 1410 kg/m^3, while the specific heat c was equal to 1,5 kJ/(kg·K). Notches consisted in a moulded central hole having a diameter equal to 10 mm characterised by an orthotropic K_t value equal to 2.84 referred to the net section. Additional tests were conduced also on notched specimens having a moulded 10 mm-wide central slit characterised by a tip radius equal to 0.5 mm and by an orthotropic K_t value equal to 7.82 referred to the net section.

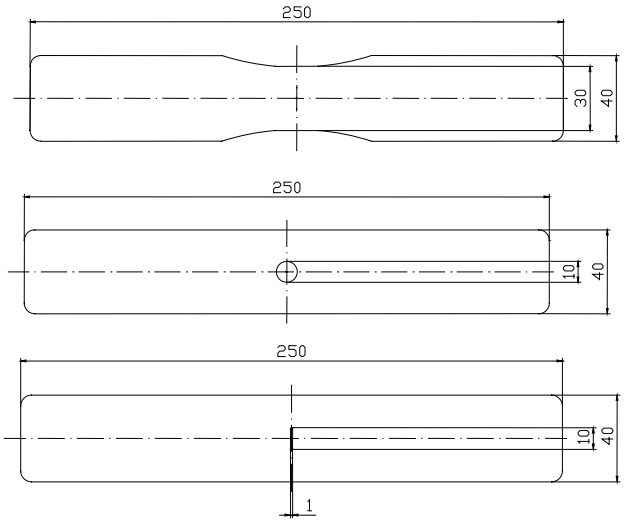

Fig. 6. Geometries of the smooth and notched specimens.

Specimens' geometries are reported in Fig. 6. Fatigue tests were conduced on a Schenck Hydropuls PSA 100 servo-hydraulic machine equipped with a 100 kN load cell. The load frequency was kept between 2 and 7.5 Hz, depending on the applied load level, while the nominal load ratio R, defined as the ratio between the minimum and the maximum applied load, was equal to 0.1. The complete separation of the specimens was assumed as failure criterion. During the tests the surface temperature of the material was monitored by means of different techniques, depending on specimen's geometry. In particular a Flir 550 infrared camera, having a resolution of 0.07 °C, was adopted for the smooth specimens, while copper-costantan (T-type) thermocouples, having 0.127 mm diameter wires and a resolution of 0.01°C, were bonded close to both the notch tips of the notched specimens. In the former case analysis and processing of the acquired frames were performed by means of the AGEMA Research 2.1 software, while in the latter case a data logger HP 34970A was adopted to sample and store the temperature signal. During the tests, the machine was suddenly stopped in order to measure the cooling gradient as a first step and then to derive the specific energy Q, according to eq. (6) and (7). The maximum adopted sampling rate was about 10 Hz when using the infrared camera and 22 Hz when using the thermocouples.

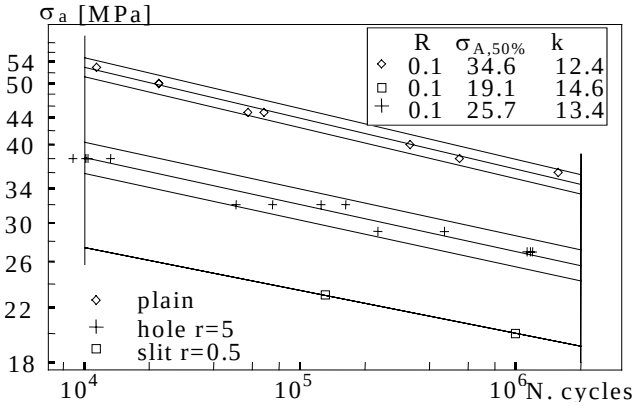

Fig. 7. Experimental fatigue test results in terms of net-section stress amplitude (r is the notch tip radius). For plain and hole specimens the 10%-90% survival probability scatter bands are also reported.

Fig. 7 reports the experimental fatigue test results in terms of net section stress amplitude σ_a. In the same figure the inverse slope k of the Woehler curve and the fatigue strength σ_A at N_A=2 million cycles for a survival probability of 50% are reported.

By comparing the σ_A values reported in Fig. 7 for the different geometries with the corresponding K_t values, it is seen that neither net-section stresses nor elastic peak stresses can correlate the experimental fatigue strength data. As an example, taking as reference stress the fatigue strength σ_A, the fatigue notch factor K_f is equal to 34.6/25.7 = 1.35 for the hole specimens, well below the elastic stress concentration factor.

5 Correlation between fatigue test results and specific energy loss Q

During the fatigue tests, 4 to 9 cooling rates and the corresponding Q values were measured after suddenly stopping the fatigue tests in order to investigate the variation of the specific energy loss Q with the number of cycles.

Fig. 8 and 9 show the typical cooling curve measured for two plain specimens in the low cycle and in the medium cycle fatigue regime, respectively.

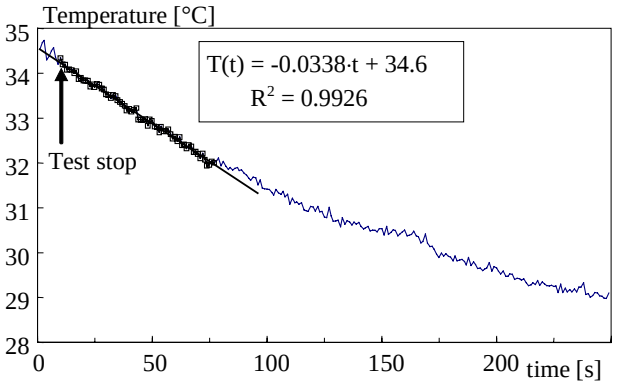

Fig. 8. Example of a cooling curve measured by means of the infrared camera for a plain specimen (σ_a=53 MPa, N/N_f=0.44, N_f=11400 cycles).

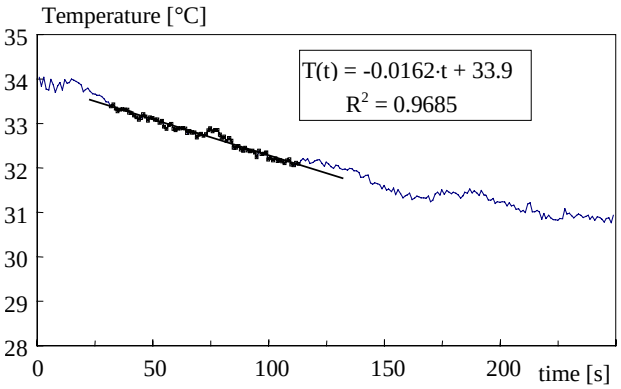

Fig. 9. Example of a cooling curve measured by means of the infrared camera for a plain specimen (σ_a=40 MPa, N/N_f=0.41, N_f=326300 cycles).

The reported markers enable one to appreciate the adopted sampling frequency equal to 1 Hz and show the set of temperature-time data that were processed in order to estimate the cooling gradient and then the specific energy Q.

When dealing with notched specimens some experimental difficulties in interpreting the cooling curves arose. In fact the temperature variations that had to be measured during the cooling phase resulted to be on the order of just few tenths of a degree, while in the case of plain specimens temperature drops of 1÷2 degree were observed, as shown by previous figures 8 and 9. That is why thermocouples having a higher resolution than the infrared camera were adopted in the case of notched specimens. The same experimental difficulty was highlighted by one of the Authors of the present work when applying the presented thermometric method to study the fatigue behaviour of metallic materials [18]. As an example , fig. 10 reports the cooling curve measured by means of thermocouples for a hole specimen. In this case the sampling rate had to be increased to 10 Hz, due to the higher decrease of the cooling gradient with respect to time.

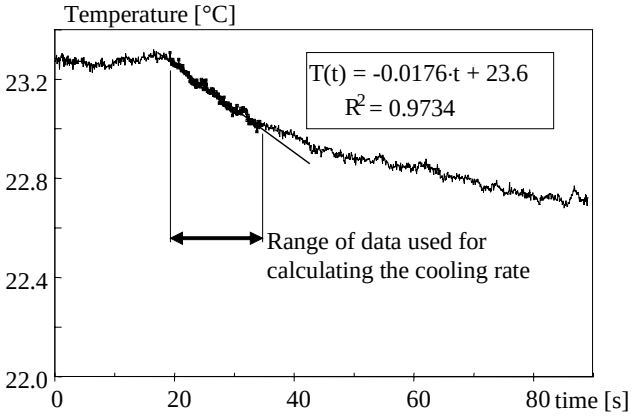

Fig. 10. Example of a cooling curve measured by means of the thermocouples for a hole specimen (r=5 mm, σ_a=32 MPa, N/N_f=0.45, N_f=162400 cycles).

Concerning the plain specimens, it has been observed that in the medium and high cycle fatigue regime the specific energy Q increases at the beginning of the test and then it remains roughly constant starting from about 40÷50% of the total fatigue life. As an example Fig. 11 reports the measured values of Q for two plain specimens which failed at N_f=68300 and N_f=326340 cycles, respectively.

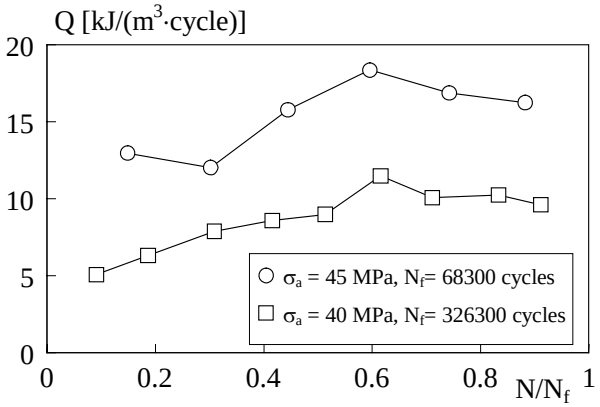

Fig. 11. Typical trend of the specific energy Q measured for two plain specimens in the medium cycle regime.

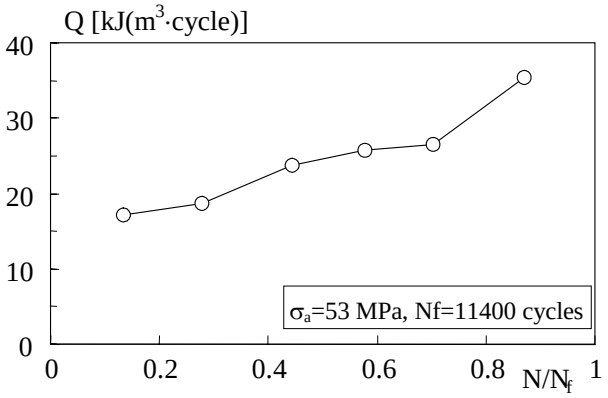

Fig. 12. Typical trend of the specific energy Q measured for a plain specimen in the low cycle fatigue regime.

Conversely in the low cycle fatigue regime the specific energy Q is more like an increasing function of the number of cycles, as shown by Fig. 12. Then in the former case the mean value after stabilization was considered as characteristic for that test, while in the latter case the value measured at 50% of the fatigue life was taken into account.

Concerning the notched specimens, it was not found a change in the behaviour in the different fatigue regimes. Fig. 13 reports as an example the specific energy loss Q as a function of the relative number of cycles. The curve is roughly constant during the whole fatigue test, then the mean value was considered as characteristic for that specimen. The same choice was done for the other analysed stress levels.

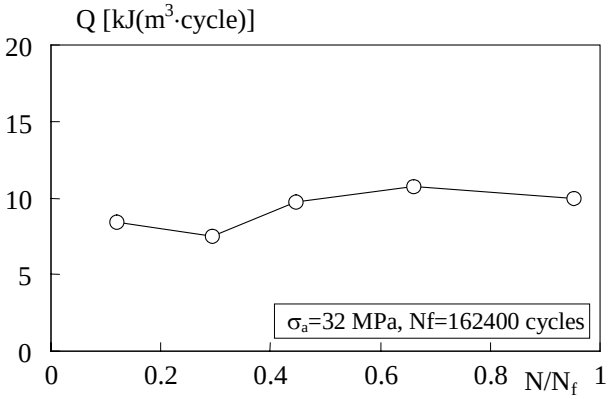

Fig. 13. Typical trend of the specific energy Q measured for a hole specimen (r=0.5 mm) in the medium cycle fatigue regime.

Similarly to the trend shown by fig. 13, the specimens containing slits showed that the energy dissipation was almost constant during the fatigue test. Unfortunately the temperature rise after the beginning of the fatigue test was limited to few tenth of a degree so that the measurements were affected by high uncertainties. One simple method for forcing higher temperature rises is to increase the load test frequency in order to increase the dissipated thermal power and then the surface temperature level. In the present case such a method was limited by the capacity of the available servo-hydraulic testing system so that it could not be effective. By re-arranging the available experimental results shown in Fig. 7 in terms of specific energy Q, the scatter bands shown by Fig. 14 were obtained.

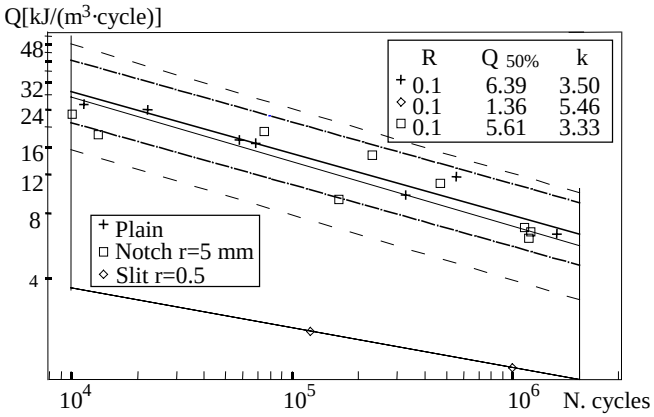

Fig. 14. Experimental fatigue test results in terms of energy Q dissipated as heat in a unit volume of material per cycle.

Fig. 14 reports all the experimental results in terms of specific energy loss Q, as calculated by means of eq. (6) and (7). It can be seen that the mean curves for to plain and hole specimens are much closer to each other than in terms of net-section stresses. Then a confidence analysis was performed in order to investigate if the results of these two test series can be treated as a single set, i.e. if the energy parameter Q can correlate the fatigue strength of the plain and smoothly notched specimens.

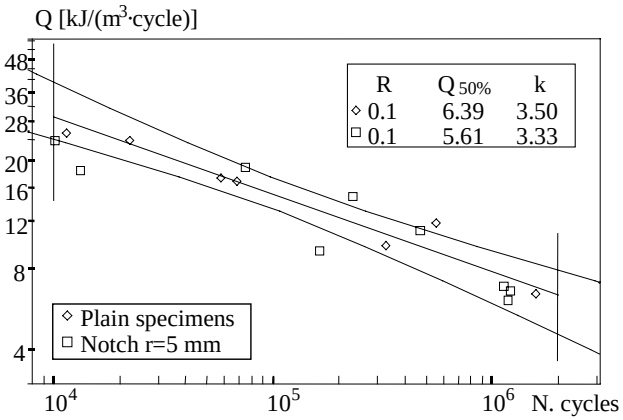

Fig. 15. Mean energy-based fatigue curve and confidence band for the plain specimens

Fig. 15 shows the mean curve and the corresponding confidence band for plain specimens. It is seen that most of the data valid for the notched specimens fall well within the confidence band. That is why all data were processed as a single test serie in Fig. 16, thus supporting the use of the energy parameter Q for summarising the fatigue strength of smooth and notched specimens, at least for the analysed material.

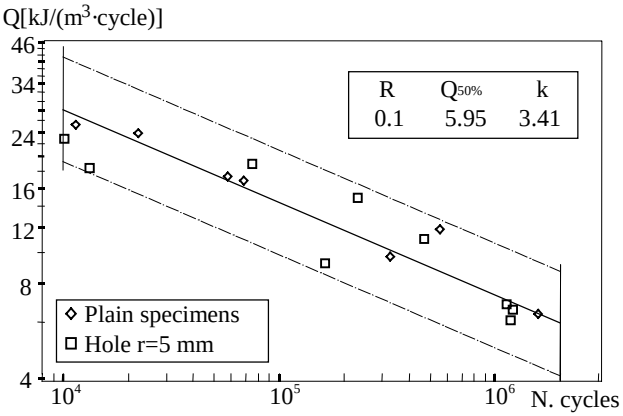

Fig. 16. Energy-based scatter band for plain and hole specimens.

6 Discussion

Fig. 14 shows that the specific energy as measured by means of the presented experimental technique cannot correlate the fatigue strength of the slit specimens having notch tip radius equal to 0.5 mm. In this case the experimental measurements as conduced in the present work are believed to be unreliable due to the very small surface thermal rise that was observed. Then the experimental technique proposed in the present work reveals some limits of applicability the sharper is the considered notch, due to the progressively weak temperature signal that are expected to be measured.

Apart from the difficulties due to the small temperature rises, it should be noted that the proposed energy parameter Q is by nature a local quantity defined at a *point* in a component. As a consequence the proposed approach is correlated to the fatigue life up to crack initiation and not to the following crack propagation phase when the crack tip moves far away from the initiation point, that is from the point where the specific energy Q is measured. As far as the fatigue life of a component is mainly spent to initiate a crack, the proposed experimental energy based approach is promising. Conversely, if a significant fraction of the fatigue life is spent to propagate a macro-crack, then parameter Q can hardly correlate fatigue data generated by notches of different geometry. The latter case holds true the sharper is the considered notch. Fig. 17 shows as an example the stiffness curves as measured for a specimen containing the hole (r=5 mm, N_f=111180 cycles) and the slit (r=0.5 mm, N_f=139000 cycles), respectively. Being the fatigue lives almost the same for the two specimens, the relative stiffness curve trends are comparable up to about 50% of the fatigue life and then the one relevant to the sharper notch drops with steeper gradients with respect to the other. That means that a longer fraction of the fatigue life is spent to propagate a crack in the case of the sharper notch. Then it is believed that the proposed method correlates only the crack initiation life obtained from different specimens' geometries. On the other hand the definition of 'crack initiation life' is beyond the purpose of the present work.

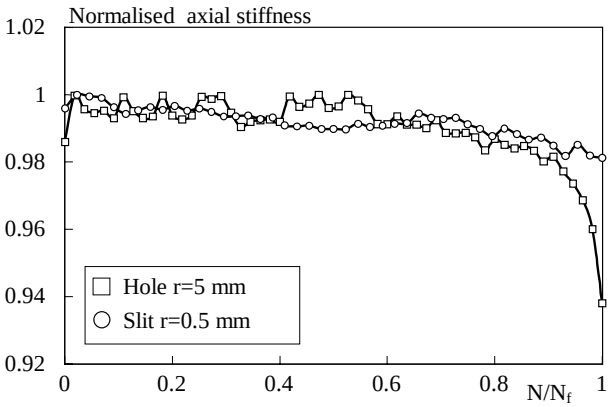

Fig. 17. Non-dimensional axial stiffness versus the relative number of cycles for two specimens having different notch tip radius.

7 Conclusions

The specific energy parameter is able to correlate the fatigue strength of plain and notched specimens, characterized by a notch tip radius equal to 5 mm, made of a 5-mm-thick PA66-GF35 material, i.e. a 35% short glass fiber reinforced polyamide composite. Then a unique scatter band where the experimental data for to both specimens' geometries collapse has been defined. Conversely, neither net-section stresses nor elastic peak stresses can correlate the fatigue strength.

Additional fatigue tests were performed by using more severely notched specimens containing a slit with a notch tip radius equal to 0.5 mm. In this case, due to the very limited thermal rise observed at

the notch tip, temperature measurements are affected by great uncertainties.

Even when adopting an experimental equipment having higher resolution than the one available in the present work, care should be paid when applying the proposed approach to severely notched specimens because the proposed energy parameter is correlated by nature only to the fatigue crack initiation life; conversely the crack propagation phase could be more and more significant the sharper the notch geometry is.

References

[1] Luong MP. "Fatigue limit evaluation of metals using an infrared thermographic technique". *Mech Mater*, 28, pp 155-163, 1988.

[2] La Rosa, G, Perrone, S, Quaresimin, M. "Fatigue strength assessment of composite materials through thermographic techniques ", *Proceedings of 27th AIAS National Conference*, Perugia - Italy pp.799-808, 1998 (*in Italian*).

[3] Quaresimin M. "Fatigue of woven composite laminates under tensile and compressive loading" - *Proceedings of 10th European Conference on Composite Materials*, Brugge, 2002.

[4] Catalbiano T, Geraci A, Orlando M. "Analysis of the fatigue strength of specimens by means of the infrared technique". *Il Progettista Industriale* 2, 1984 (in Italian).

[5] Neubert H, Schulte K, Harig H. "Evaluation of the damage development in carbon fiber reinforced plastics by monitoring load-induced temperature changes". *Composite Materials: Testing and Design (Ninth Volume) ASTM STP 1059*, pp. 435-453, 1990.

[6] Curà F, Curti G, Sesana R. "A new iteration method for the thermographic determination of fatigue limit in steels". *Int. J. Fatigue*, 27, pp 453-459, 2005.

[7] Kaleta J, Blotny R, Harig H. "Energy stored in a specimen under fatigue limit loading conditions". *J Test Eval*, 19, pp. 326-333, 1990.

[8] Cugy P, Galtier A. "Microplasticity and temperature increase in low carbon steels". *Fatigue 2002: Proceedings of the 8th International Fatigue Congress*, Vol. I, EMAS, pp. 549-556, 2002.

[9] Miller KJ. "The three thresholds for fatigue crack propagation" *ASTM STP 1296*, pp. 267-286, 1997.

[10] Murakami Y. "*Metal fatigue: effects of defects and non metallic inclusions*" Elsevier, 2002.

[11] Reifsnider KL, Williams RS. "Determination of fatigue-related heat emission in Composite materials". *Exp Mech*, 14, pp 479-485, 1974.

[12] Quaresimin, M. Guglielmino, E. , "Static notch sensitivity of GFRP composites", *Key Engineering Materials*, 221-222, pp.121-132, 2002.

[13] Gamstedt EK, Redon O, Brønsted P. "Fatigue Dissipation and Failure in Unidirectional and Angle-Ply Glass Fibre/Carbon Fibre Hybrid Laminates", *Key Eng Mat*, vols 221-222, pp 35-48, 2002.

[14] Mian A, Han X, Sarwar Islam S, Newaz G. "Fatigue damage detection in graphite/epoxy composites using sonic infrared imaging technique". *Compos Sci Technol* 64, pp. 657–666, 2004.

[15] Bellenger V, Tcharkhtchi a., Castaing Ph. "Thermal and mechanical fatigue of a PA66/glass fibers composite material". *Int. J. Fatigue*, 28, pp 1348-1352, 2006.

[16] Steinberger R, Valadas Leitão T.I, Ladstätter E, Pinter G, Billinger W, Lang R.W. "Infrared thermographic techniques for non-destructive damage characterization of carbon fibre reinforced polymers during tensile fatigue testing". *Int. J. Fatigue*, 28, pp 1340-1347, 2006.

[17] Toubal L, Karama M., Lorrain B. "Damage evolution and infrared thermography in woven composite laminates under fatigue loading". *technical note Int. J. Fatigue*, 28, pp 1867-1872, 2006.

[18] Meneghetti G. "Analysis of the fatigue strength of a stainless steel based on the energy dissipation". *Int. J. Fatigue*, 29, pp 81-94, 2007.

[19] Feltner CE, Morrow JD. "Microplastic Strain Hysteresis Energy as a Criterion for Fatigue Fracture". *Trans. ASME, Series D, J Basic Engineering*, 83, pp. 15-22, 1961.

[20] Halford GR. "The energy required for fatigue". *J Mat*, 1, pp. 3-18, 1966.

[21] Charkaluk E, Bignonnet A, Costantinescu A, Dang Van K. "Fatigue design of structures under thermomechanical loadings". *Fatigue Fract Engng Mater Struct* 25, pp. 1199-1206, 2002.

[22] Klingbeil NW. "A total dissipated energy theory of fatigue crack growth in ductile solids". *Int J Fatigue* 25, pp.117-128, 2003

[23] La Rosa G, Risitano A. "Thermographic methodology for rapid determination of the fatigue limit of materials and mechanical components". *Int. J. Fatigue*, 22, pp 65-73, 2000.

[24] Fargione G, Geraci A, La Rosa G, Risitano A. "Rapid determination of the fatigue curve by the thermographic method". *Int J Fatigue*, 24 pp. 11-19, 2002.

[25] Atzori B, Gasparini E, Meneghetti G. "Thermographic analysis of the fatigue strength of metallic materials" - *Proceedings of 30th AIAS National Conference*, Alghero - Italy pp. 367-376, 2001 (*in Italian*).